Inversion Recovery Cross-Polarization NMR in Solid Semicrystalline Polymers

D. G. Cory* and W. M. Ritchey

Department of Chemistry, Case Western Reserve University, Cleveland, Ohio 44106.
Received December 30, 1986; Revised Manuscript Received August 22, 1988

ABSTRACT: Crystalline and amorphous components of polyethylene and poly(oxymethylene) were resolved from differences in their cross-polarization rates by ^{13}C inversion recovery cross-polarization NMR, IRCP, with magic angle sample spinning and high-power proton decoupling at 15.1 MHz. IRCP differs from other relaxation methods employed to resolve morphological differences; signals from each component go through a null, and more rigid components may be unambiguously assigned to those with faster cross-polarization rates. The degree of crystallinity of the polymers and the line widths and chemical shifts of each component are reported and agree with previous results.

Introduction

Since the combination of cross-polarization, magic angle sample spinning, MAS, and high-power proton decoupling by Schaefer and Stejskal[1] to obtain high-resolution NMR of solids, considerable effort has been expended to achieve greater resolution. In attempts to resolve morphological differences in polymers, attention has naturally been focused on methods which discriminate on the basis of relaxation phenomena, since changes in morphology normally are accompanied by changes in molecular dynamics which are reflected in relaxation times.[2] When crystalline components are resolved from amorphous components, three points should be kept in mind: one would prefer to observe each component separately (ideally without performing spectral subtractions), to unambiguously assign the components, and to do so with good signal to noise. While the success in achieving these goals depends somewhat on the polymer of interest, general characteristics of various relaxation measurements may be noted. The relaxation times commonly studied include the spin–lattice relaxation time, T_1; the rotating frame spin–lattice relaxation time, $T_{1\rho}$; the dipolar dephasing time, T_{DD}; and the cross-polarization time, T_{CH}. While T_1 measurements may be performed by an inversion–recovery method which selectively nulls each component and hence allows the other component to be observed separately, the other relaxation parameters are normally measured via a decay in the signal. Deviations from exponential behavior are indications of multiple components, and provided that the relaxation times are sufficiently different, one may selectively observe the resonance of the more slowly decaying component. The resonance of the faster decaying component is then obtained by spectral subtraction from the original spectrum. T_1 measurements which avoid spectral subtraction often lead to long experimental times since the T_1's of crystalline solids are often long.

It is not trivial to unambiguously assign resonances as crystalline or amorphous based solely on a measured relaxation time. For T_1 relaxation, one must know which side of the relaxation dispersion curve one is on, and this will depend on the Larmor frequency. $T_{1\rho}$ relaxation times may only be assigned directly when spin–spin effects may be ignored. Spin–spin interactions can cause the $T_{1\rho}$ of the crystalline component to be greatly reduced, unless large spin-lock fields are employed. T_{DD} and T_{CH} may almost always be unambiguously interpreted unless very mobile materials are being studied in which the effects of MAS cannot be ignored (i.e., adamantane).

Melchior[3] has developed an inversion–recovery cross-polarization, IRCP, sequence which discriminates on the basis of the cross-polarization time, T_{CH}, and may be used to selectively null overlapping resonances. This has the potential of fulfilling all three of the above requirements. Each component may be selectively nulled to yield a spectrum of the other without spectral subtractions. The more quickly cross-polarizing component is the crystalline, and since both cross-polarization times are relatively short, sensitivity is not lost. This study employs IRCP methods to characterize the crystallinity of polyethylene, PE; and poly(oxymethylene), POM. Both of these polymers are semicrystalline and have been widely studied by solid-state NMR. Under normal CP/MAS conditions, they both yield single resonances which may be resolved into at least two components by a variety of relaxation methods.

Experimental Section

The NMR spectrometer is home built around a Varian 60-MHz (1.4-T) electromagnet and a Nicolet 1180 computer with 293B pulse programmer. The spin-lock fields employed have rotating amplitudes matched at 71 kHz and were generated with Chemagnetics amplifiers. The magic angle sample spinner is Gay's[4] design and spins stably from 500 to 2500 Hz. The POM sample was machined as a 5-mm rod, and the PE sample was packed as a powder into a cut-off 5-mm NMR tube. The rotor is machined from Delrin but is not observed since it is surrounded by brass from the stator. The electronics of the probe utilize bulk tuning elements and are similar to those described by Bartuska and Maciel.[5]

IRCP experiments, shown in Figure 1, were run with 13 τ_2 values from 10 μs to 1 msec, and a τ_1 of 2 ms. The acquisitions were automated with 2 sets of 1024 transients being accumulated and averaged to suppress effects of slow drift during the experiments. This experiment is particularly sensitive to variations in the Hartmann–Hahn condition. Immediately upon completion of the experiment, the data were analyzed to yield the cross-polarization rates, and two additional experiments were performed with τ_2 values corresponding to T_{CH} ln 2 for each component. This condition should suppress the component associated with the measured cross-polarization time. All results reported here were obtained by inverting the spin temperature with a phase shift of the proton spin-locked field, Figure 1A. Additional phase shifting is also used to implement spin temperature alternation[6] which eliminates Bloch decay components and phase glitches. This is accomplished by inverting the phase of the proton 90° pulse on every other acquisition and alternately adding and subtracting the resultant free induction decays (fid).

The POM sample was obtained commercially as Delrin, and the PE is a low-density sample from Aldrich.

Results

Both POM[7–9] and PE[10–14] are well characterized by solid-state NMR techniques; the purpose of this study was to determine the utility of IRCP as a method of resolution enhancement in high-resolution MAS NMR. Two versions of the pulse sequence are shown in Figure 1. While IRCP may be applied more generally, we will restrict our discussion to the case where the first cross-relaxation time,

* Present address: Code 6120, Chemistry Division, Naval Research Laboratory, Washington, DC 20375-5000.

0024-9297/89/2222-1611$01.50/0

Table I
Poly(oxymethylene)[a]

relaxation process	T_{CH}	$T_{1\rho}$[7]	T_1[8]	T_1[8]	NOE[8]	T_{DD}[9]
field strength	71 kHz	25 kHz	45 MHz	15 MHz	15 MHz	
crystallinity	69%	70%	(63% by X-ray)			
relaxation times						
crystalline	13 μs	1.5 ms	15 s	1.5 s	1.3	7 μs
amorphous	290 μs	17.5 ms	75 ms	50 ms	1.6	92 μs
chem. shift diff.	0.85 ppm	1 ppm				1 ppm
line width						
crystalline	52 Hz					
amorphous	57 Hz					

[a] The accuracy of the relaxation measurements is ±10%, though statistically the error is much smaller. The chemical shift difference is accurate to ±0.1 ppm and the line width to ±1 Hz, but the contribution from the static field inhomogeneity is much greater (about 5–10 Hz). The error in the crystallinity measurement is more difficult to quantify since dividing the sample into only crystalline and amorphous regions is likely an oversimplification. The agreement of the three different measurements is an indication of their accuracy.

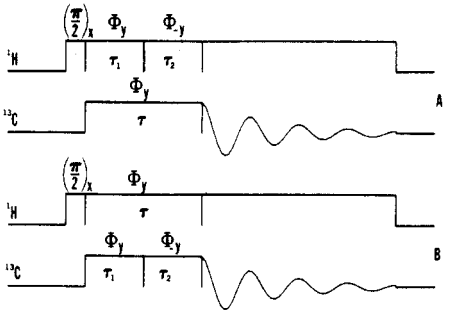

Figure 1. Pulse sequence for IRCP T_{CH} measurements with spin temperature inversion on the proton, sequence A, and carbon, sequence B. All of our results were obtained with sequence A.

τ_1, is much longer than any cross-polarization time, T_{CH}, observed in the sample. This first period then becomes analogous to the 90° pulse in an inversion–recovery method for measuring spin–lattice relaxation times in solution[15] and is simply used to generate a large magnetization. After time τ_1, the spin temperature of either the proton or carbon reservoir is inverted, by changing the phase of the spin-lock field by 180°. If we assume that the proton heat capacity is infinite, then in both cases the carbon inverse spin temperature must go through zero before returning to equilibrium with the proton reservoir. The observed magnetization follows the inverse spin temperature, and τ_2 becomes analogous to the time between the 180° and 90° pulses in an inversion–recovery sequence. The magnetization recovers with a time constant of T_{CH}.

Poly(oxymethylene). Figure 2 shows the IRCP results for POM, a linear polymer in which all carbons are chemically equivalent. The normal CP/MAS spectrum yields a resonance at 89 ppm downfield from TMS with a width of about 3 ppm. It has been shown by Veeman et al.[7] that the peak is actually composed of two resonances. They are separated by about 1 ppm, with the narrower crystalline component appearing at higher field. The magnetization clearly inverts and does so with a double-exponential dependence. One may observe in the 30–75-μs spectra that a peak at higher field than the bulk peak inverts first, and then at longer times the low field peak also inverts. A logarithmic plot of the integrated areas of each spectrum is shown in Figure 3 along with the least-squares fit to eq 4. The double-exponential character of the relaxation is obvious; the two measured values of T_{CH} are 13 and 290 μs. The insert in Figure 3 shows an expansion of the short time behavior.

The T_{CH} is dependent on the mismatch of the Hartmann–Hahn condition which is generally not known, making quantitative comparisons difficult. For proton-rich materials which are fairly rigid and therefore have short T_{CH}'s, this effect is small, however, and variations in T_{CH} will only be observed under extreme conditions of mismatch.

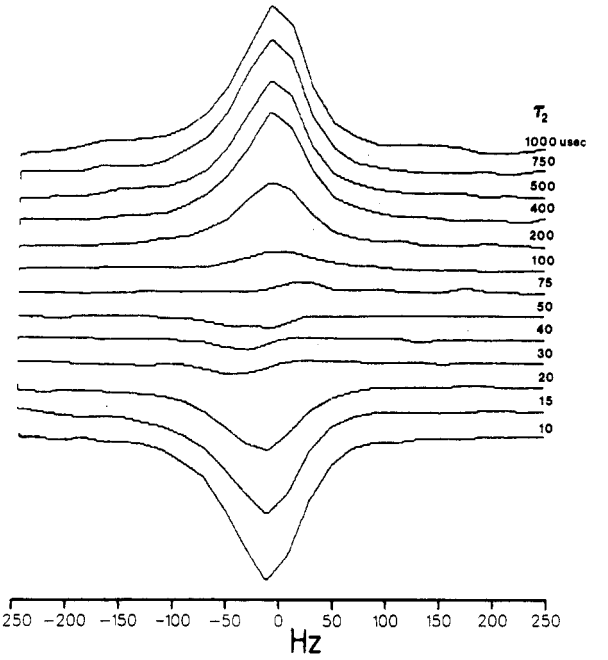

Figure 2. IRCP spectra of POM; τ_1 = 2 ms and 2048 acquisitions were collected.

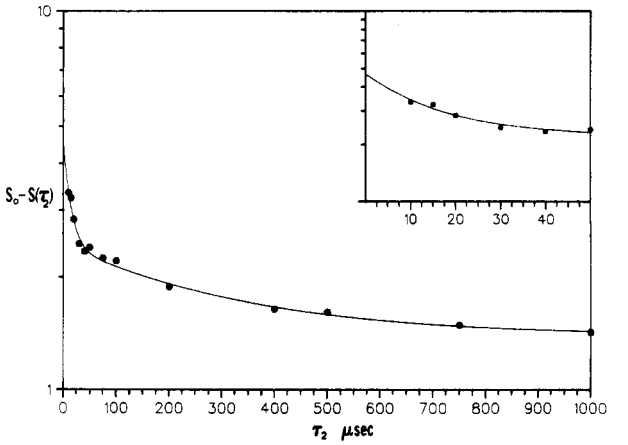

Figure 3. Logarithmic plot of the integrated peak areas from IRCP of POM in arbitrary units. The insert is an expansion of the short time behavior. The solid line is the result of a least-squares fit to eq 4.

The two separated components of POM are plotted in Figure 4, and their chemical shifts and line widths are given in Table I. The resonance of the crystalline component, Figure 4B, is shifted 0.85 ppm to higher field than

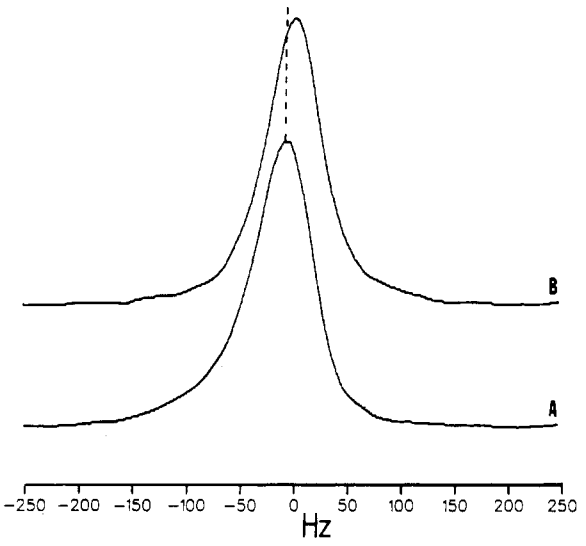

Figure 4. IRCP spectral separation of the two components of POM. Spectrum B is the crystalline component, and A is the amorphous. The phase of spectrum A is inverted from the sense of Figure 4B and Figure 2.

Table II
Polyethylene[a]

amorphous line width	26 Hz
crystalline line width	19 Hz
chem. shift diff.	0.4 ppm
T_{CH} amorphous	310 μs
T_{CH} crystalline	14 μs
% crystallinity	63%

[a] The error and accuracy of these values are the same as those given in Table I.

the amorphous component, Figure 4A, and is slightly narrower, 52 Hz as compared with 57 Hz, at 1.4 T.

Polyethylene. Figure 5 is the logarithmic plot of the integrated intensities and the least-squares fit for an IRCP study of low-density PE. As in the case of POM, both a short and long time dependence on the intensity is observed. The short time behavior is expanded in the insert. The measured time constants are 14 and 310 μs, for the crystalline and amorphous regions, respectively. Additional spectra, in which the evolution period was set to T_{CH} ln 2 for these time constants, were also run, and their chemical shifts and line widths are reported in Table II.

Data Reduction. An expression for the magnetization of an IRCP experiment may be determined by following Mehring[16] as

$$M(\tau_1,\tau_2) = M_0\left\{1 - 2\exp\left(\frac{-\alpha\tau_2}{T_{CH}}\right) + \exp\left(\frac{\alpha\tau}{T_{CH}}\right)\right\}\exp\left(\frac{\alpha\tau}{T^H_{1\rho}}\right) \quad (1)$$

where

$$\alpha = 1 - T_{CH}/T^H_{1\rho}$$

$$\tau = \tau_1 + \tau_2$$

$T^C_{1\rho}$ effects are neglected since $T^C_{1\rho} \gg T_{CH}$. If we restrict ourselves to the case where $\tau_1 \gg T_{CH}$ and $\tau < T^H_{1\rho}$, then for a two-component system

$$M(\tau_2) = M_A + M_B - 2M_A\exp(-\tau_2/T^A_{CH}) - 2M_B\exp(-\tau_2/T^B_{CH}) \quad (2)$$

or

$$\frac{\{M_0 - M(\tau_2)\}}{2} = M_A\exp\left(\frac{-\tau_2}{T^A_{CH}}\right) + M_B\exp\left(\frac{-\tau_2}{T^B_{CH}}\right) \quad (3)$$

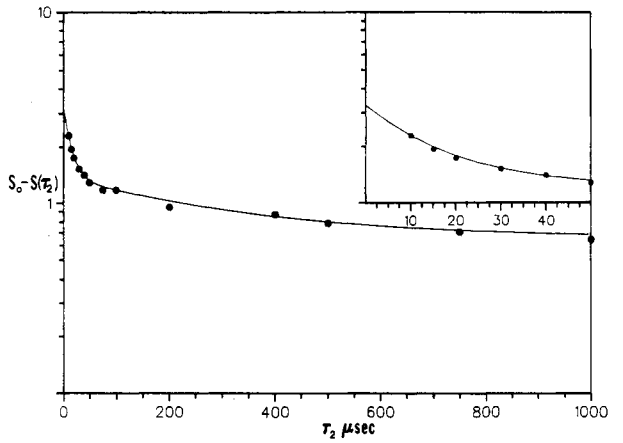

Figure 5. Logarithmic plot of the integrated peak areas from IRCP of PE in arbitrary units. The insert is an expansion of the short time behavior, and the solid line is the result of a least-squares fit to eq 4.

The quantities $\{M_0 - M(\tau_2)\}$ are plotted versus τ_2 in Figures 3 and 5, along with the least-squares fit to the function

$$S(\tau_2) = S_A\exp(-\tau_2/T^A) + S_B\exp(-\tau_2/T^B) + S_0 \quad (4)$$

Ideally S_0 should equal zero and $S(\tau_2)$ should approach zero as τ_2 becomes large. This is not observed since the decay of the proton spin-locked magnetization characterized by $T^H_{1\rho}$ may not be completely ignored. We can rewrite eq 3 assuming a linear correction for the $T^H_{1\rho}$ term as

$$\frac{\{M_0 - M(\tau_2)\}}{2} = M_A\exp\left(\frac{-\tau_2}{T^A_{CH}}\right) + M_B\exp\left(\frac{-\tau_2}{T^B_{CH}}\right) + M_0\left(\frac{\tau}{T^H_{1\rho}}\right) \quad (5)$$

S_0 of eq 4 may then be equated with the last term of eq 5 and is a measure of the importance of the $T^H_{1\rho}$ term.

Discussion

The dependence of the cross-polarization rate on molecular structure[16,17] and dynamics[19] has been reported. The cross-polarization rate follows the expression[16-19]

$$1/T_{CH} \propto M^2_{IS}J_x(\delta\omega)$$

where M^2_{IS} is the width of the carbon–proton dipolar interaction, J_x is the power density and $\delta\omega$ is the mismatch of the Hartmann–Hahn condition.

The power density is the Fourier transformation of a normalized correlation function, C_x, for the proton spins which, in the absence of motion and under only constant fields, reduces to the fid of the protons. In the rigid lattice extreme,[16-18] C_x may be written as a summation over the protons of autocorrelation and cross-correlation terms for the proton spins with a spatial dependence of $(1 - 3\cos^2\vartheta)/r^3$. Here ϑ is the angle the carbon–proton vector makes with the static field, and r is the carbon–proton distance. To a first approximation, the normalization function of C_x cancels the spatial dependence of M^2_{IS}.[18] Thus, the most significant spatial term, and the most important motional term, in the expression for $1/T_{CH}$ is J_x. It is not likely that for the data presented here giving C_x as a set of lattice sums or expanding it with a model for the motion will lead to any further information. We will limit ourselves to assuming that C_x is Gaussian,[16] resulting in a power density of

$$J_x(\delta\omega) \propto \tau_c \exp\left(\frac{-\delta\omega^2\tau_c^2}{4}\right)$$

or

$$\frac{1}{T_{CH}} \propto M_{IS}^2\tau_c \exp\left(\frac{-\delta\omega^2\tau_c^2}{4}\right)$$

where τ_c is a correlation time governing the proton–proton fluctuations. A very strongly coupled, proton-rich static material has a short τ_c, whereas a material in which rapid motions at least partially quench the coupling (or proton flip–flop process) has a longer τ_c. The exponential normally dominates the expression for the cross-polarization rate.

The situation may become more complicated, particularly in MAS studies of materials with small proton–proton second moments, for example, adamantane, where the cross-polarization rate is an oscillatory function of the mismatch.[20] It is well established, though, that for most solids rigid systems cross-polarize more rapidly than mobile ones, all else being the same.

Since IRCP depends on accurately nulling a component based on its T_{CH}, the effects of the expected distribution of relaxation times must be considered. The resulting errors from a distribution of relaxation times will be more pronounced in inversion–recovery methods (i.e., T_1 and T_{CH}) than in simple decay methods (i.e., $T_{1\rho}$ and T_{DD}). Pines et al.[21] and Naito et al.[22] have observed distributions of relaxation times in solid samples and have noted that, even though they arise from orientation effects, MAS will not completely remove these. Naito et al. point out that, since the spinner period is short compared to T_1, the distribution in T_1 may be calculated by averaging the relaxation rate in cylinderical coordinates. They found that for a number of amino acids, the effects of a distribution of the relaxation times could be observed, but that they were small. In the more demanding sample of solid benzene,[21] the distribution is larger.

The case of T_{CH} is more complicated since it is, in general, shorter than the spinner period, and thus averages of the type performed by Naito et al. are no longer valid. Here the anisotropy is averaged primarily by molecular motions. Again for solid benzene,[21] a distribution of T_{CH}'s has been observed, and the geometric factor for T_{CH} has been derived. The angular dependence of the relaxation rate goes as $(1 - 3\cos^2\vartheta)$, where ϑ is the angle the C–H dipolar pair makes to the static field. For proton-rich samples, the number of contributing cross-relaxation pathways for T_{CH} eliminate much of its inherent anisotropy. T_1 relaxation normally is dominated by a small number of rapidly reorienting groups (i.e., methyls) since for relaxation to be efficient there must be components of the spectral density at the Larmor frequency. In the case of T_{CH}, all that is required is that a dipolarly coupled C–H pair have a coupling greater than the mismatch of the Hartmann–Hahn condition. For well-matched radio-frequency fields, near nonbonded protons as well as those bonded contribute with relaxation rates scaled by the proton–proton fluctuation time. For the polymers studied, each carbon atom is bonded to two protons, and only small distributions of relaxation times are observed. The inversion–recovery curves are described well by a double-exponential behavior.

Veeman and co-workers[7,8] have shown that POM undergoes rapid motions in both the crystalline and amorphous states, though the amplitude of the motion for the crystalline is very restricted compared to the amorphous. These motions also help to average out the distribution of relaxation times expected for T_{CH}.

Even in the case of PE where less motion is expected, the inversion–recovery curves are well described by a biexponential. VanderHart[23] has observed variations in T_{CH} with orientation in nonspinning single-crystal studies of *n*-eicosane, a 20-carbon model compound for PE. Motional averaging in the single crystal is far less than in the samples studied here. The large differences in relaxation times (14 compared to 310 μs) help to mask these small distributions. Schröter and Posern[11] have observed four components in PE based on studies of T_1, two each for the amorphous and crystalline fractions. We do not observe such effects in these studies, and it is likely that the T_{CH} is not as sensitive to the changes in dynamics associated with these components as is the T_1. Cross-relaxation occurs so rapidly that only motions which reduce the dipolar coupling greatly affect the cross-relaxation rate.

The short time behavior of IRCP must also be considered since one might reasonably expect transient oscillations on the same time scale as the crystalline relaxation rate.[24,25] Transient oscillations arise from a rapid change in the Hamiltonian of tightly coupled spin systems, occur at a frequency characteristic of the new Hamiltonian, and decay at a rate following the line width. In the nonordered systems reported on here, it would be difficult to observe these oscillations since each orientation behaves differently. We have, however, looked for them with a single-crystal sample and have failed to observe any oscillations within the sensitivity of the experiment (about 20%). If the experiment is performed properly, transient oscillations should not be observed since the eigenstates of the Hamiltonian prior to inverting the spin temperature are still good states after the inversion is complete. The system should simply approach thermal equilibrium monotonically.

The time constant associated with the dipolar dephasing experiment, T_{DD},[26] and IRCP are similar in origin, and one may expect to obtain information from their ratio.

Conclusions

IRCP is a useful method of generating separate spectra for the various morphological components of semicrystalline polymers. It usually requires less experimental time than other relaxation methods and yields spectra from both components without spectral subtractions. The degree of crystallinity, line widths, and positions may be easily measured, and the crystalline component may be unambiguously assigned to the faster relaxing signal. While at this time the T_{CH} does not enjoy the ease of quantitative interpretation that is associated with T_1 or T_2 relaxation times, differences may readily be explained in terms of proton density and mobility, and the IRCP technique is an accurate method of measuring T_{CH}. It is anticipated that for many solid polymers the T_{CH}'s will be sufficiently short to be insensitive to the Hartmann–Hahn mismatch in a well-tuned spectrometer. For proton poor samples and very mobile materials, some care should be taken to understand the effects of mismatch on the result.

Acknowledgment. We thank Dr. M. Melchior and Dr. W. S. Veeman for very helpful discussions. Support from the Standard Oil Co. (Ohio) is gratefully acknowledged.

Registry No. PE, 9002-88-4.

References and Notes

(1) Schaefer, J.; Stejskal, E. O. *J. Am. Chem. Soc.* **1976**, *98*, 1031.
(2) Zumbulyadis, N. *J. Magn. Reson.* **1983**, *53*, 486.
(3) Melchior, M. T., private communication.

(4) Gay, I. D. *J. Magn. Reson.* **1984**, *58*, 413.
(5) Bartuska, V. J.; Maciel, G. E. *J. Magn. Reson.* **1981**, *42*, 312.
(6) Stejskal, E. O.; Schaefer, J. *J. Magn. Reson.* **1975**, *18*, 560.
(7) Veeman, W. S.; Menger, E. M.; Ritchey, W.; de Boer, E. *Macromolecules* **1979**, *12*, 924.
(8) Menger, E. M.; Veeman, W. S.; de Boer, E. *Macromolecules* **1982**, *15*, 1406.
(9) Cholli, A. L.; Ritchey, W. M.; Koenig, J. L. *Spectrosc. Lett.* **1983**, *16*, 21.
(10) Earl, W. L.; VanderHart, D. L. *Macromolecules* **1979**, *12*, 762.
(11) Schröter, B.; Posern, A. *Makromol. Chem., Rapid Commun.* **1982**, *3*, 623.
(12) Axelson, D. E. *J. Polym. Sci., Polym. Phys. Ed.* **1982**, *20*, 1427.
(13) Dechter, J. J.; Komoroski, R. A.; Axelson, D. E.; Mandelkern, L. *J. Polym. Sci., Polym. Phys. Ed.* **1981**, *19*, 631.
(14) Fyfe, C. A.; Lyerla, J. R.; Volksen, W.; Yannoni, C. S. *Macromolecules* **1979**, *12*, 757.
(15) Farrar, T. C.; Becker, E. D. *Pulsed and Fourier Transform NMR*; Academic Press: New York, 1971; p 20.
(16) Mehring, M. *Principles of High Resolution NMR in Solids*, 2nd ed.; Springer-Verlag: New York, 1983.
(17) Demco, D. E.; Tegenfeldt, J.; Waugh, J. S. *Phys. Rev. B* **1975**, *11*, 4133.
(18) (a) Alemany, L. B.; Grant, D. M.; Pugmire, R. J.; Alger, T. D.; Zilm, K. W. *J. Am. Chem. Soc.* **1983**, *105*, 2133. (b) *Ibid.* **1983**, *105*, 2142.
(19) Cheung, T. T. P.; Yaris, R. *J. Chem. Phys.* **1980**, *72*, 3604.
(20) Stejskal, E. O.; Schaefer, J.; Waugh, J. S. *J. Magn. Reson.* **1977**, *28*, 105.
(21) Pines, A.; Gibby, M. G.; Waugh, J. S. *J. Chem. Phys.* **1973**, *59*, 569.
(22) Naito, A.; Ganapathy, S.; Akasaka, K.; McDowell, C. A. *J. Magn. Reson.* **1983**, *54*, 226.
(23) VanderHart, D. L. *J. Chem. Phys.* **1976**, *64*, 830.
(24) VanderHart, D. L.; Garroway, A. N. *J. Chem. Phys.* **1979**, *71*, 2773.
(25) Mansfield, P.; Richards, K. H. B.; Ware, D. *Phys. Rev. B* **1970**, *1*, 2048.
(26) Alemany, L. B.; Grant, D. M.; Alger, T. D.; Pugmire, R. J. *J. Am. Chem. Soc.* **1983**, *105*, 6697.

High-Resolution Solid-State ^{13}C Nuclear Magnetic Resonance Spectroscopy of Tunicin, an Animal Cellulose

P. S. Belton and S. F. Tanner*

A. F. R. C., Institute of Food Research, Colney Lane, Norwich NR4 7UA, United Kingdom

N. Cartier and H. Chanzy

Centre de Recherches sur les Macromolécules Végétales,† C.N.R.S., B.P 68, 38402, Saint Martin d'Hères, Cedex, France. *Received May 24, 1988; Revised Manuscript Received September 27, 1988*

ABSTRACT: High-resolution solid-state ^{13}C NMR spectra have been obtained from tunicin, a highly crystalline cellulose of animal origin. The spectra of this material contained relatively narrow lines, and peak multiplicities were observed at C1, C4, and C6. Two-component multiplets at C1 and C4 indicate that tunicin consists principally of the Iβ allomorph (as defined by VanderHart and Atalla). The spectrum of tunicin was compared with those recorded from *Valonia ventricosa* and the crystalline regions of cotton.

Introduction

The crystal structure of native cellulose (Cellulose I) has been investigated by using both X-ray and electron diffraction techniques.[1-3] More recently, a number of studies have employed high-resolution solid-state ^{13}C NMR to obtain structural information on cellulose. The appearance of ^{13}C resonances assigned to crystalline or highly ordered regions of native cellulose is variable and depends on sample origin. Peak multiplicities have been observed (particularly at C1 and C4) and three theories have been proposed to account for the spectral variability and the splitting patterns.[4-6] VanderHart and Atalla[4] have suggested that the more ordered component of native cellulose is composed of two allomorphs, Iα and Iβ, and that any native cellulose can be made up of varying amounts of these two forms. The Iα form gives an intense single line at C1 and a doublet at C4, while Iβ gives doublets at both C1 and C4. Thus, the ^{13}C spectrum of an algal cellulose isolated from *Valonia ventricosa* consists of three-component multiplets at C1 and C4 due to the overlap of resonances arising from the two allomorphs. NMR experiments isolating the more crystalline components of cotton suggest that the native cellulose occurring in higher plants is principally in the Iβ form. Further, the C4 line shape of the Iβ allomorph was probably more complicated than had originally been proposed.[7] Cael et al.[5] have proposed a different model for the interpretation of native cellulose spectra which is based on diffraction data. They suggest that cellulose consists of varying amounts of material characterized by either eight or two chain unit cells. The two-chain cell gives a two-component 1:1 multiplet, while the eight-chain cell gives a "triplet" with an intensity ratio of 1:2:1. *V. ventricosa* contains only eight-chain unit cell material and, according to the model, gives a three-component multiplet at both C1 and C4. The intense central component arises from four similar chains labeled A, B, C, and D, and the surrounding weaker peaks are assigned to two chains labeled E and F.

In this report, we present the high-resolution ^{13}C spectrum of a native cellulose isolated from pelagic tunicates. This spectrum is the first to be obtained from cellulose of animal origin. The tunicate cellulose (hereafter referred to as tunicin) is of special interest because its preparation requires only mild chemical and enzymic treatment. This is in marked contrast to the severe treatment carried out on low DP regenerated cellulose,[4] a material giving a similar spectrum to tunicin. Examination of tunicin using an electron microscope shows that it is highly crystalline[8] and consists of randomly intertwined cellulose microfibrils.[9] These microfibrils are approximately 10 nm in width, and like *V. ventricosa*, each tunicin microfibril is a distinct cellulose crystal having the full width of the microfibril.[10] Tunicin cellulose is less crystalline than *V. ventricosa* but

† Affiliated with the Joseph Fourier University of Grenoble.

0024-9297/89/2222-1615$01.50/0